LA-UR-12-24430
Approved for public release; distribution is unlimited.

Title:	A Fiber Interferometer for the Magnetized Shock Experiment
Author(s):	Yoo, Christian
Intended for:	final report National Undergraduate Fellowship Report

Christian Yoo
PPPL NUF Final Report
LA-UR-12-24184

A Fiber Interferometer for the Magnetized Shock Experiment

Abstract

The Magnetized Shock Experiment (MSX) at Los Alamos National Laboratory requires remote diagnostics of plasma density. Laser interferometry can be used to determine the line-integrated density of the plasma. A multi-chord heterodyne fiber optic Mach-Zehnder interferometer is being assembled and integrated into the experiment. The advantage of the fiber coupling is that many different view chords can be easily obtained by simply moving transmit and receive fiber couplers. Several such fiber sets will be implemented to provide a time history of line-averaged density for several chords at once. The multiple chord data can then be Abel inverted to provide radially resolved spatial profiles of density. We describe the design and execution of this multiple fiber interferometer.

Table of Contents

1. Introduction
    a. Overview of MSX
        i. What is MSX?
        ii. Why MSX?
        iii. How does MSX work?
    b. Brief description of the principles of interferometry
    c. Significance of the application of this interferometer to MSX
2. Experiment
    Description of the interferometer apparatus and its components
3. Physics and Mathematics of the apparatus
    a. Mirrors
    b. AOM
    c. Optical fibers
    d. Photodiode
    e. Bias Circuit
    f. Detection circuit
        i. I&Q detection
        ii. Extraction of phase shift information from the electrical signal
        iii. Abel-Inversion
        iv. Residual phase differences
    g. Sources of noise
4. Results
    a. Testing and Trouble-shooting
    b. Experimental results
5. Conclusion
6. Acknowledgements
7. References

1. Introduction

a. Overview of MSX

i. What is MSX?

MSX investigates the physics of collisionless-shocks and particle acceleration. What is a shock? A shock is what happens in a fluid-like medium when fluid flow is faster than the local characteristic wave speed (e.g. sonic speed) for the medium. There is a boundary where flow transitions from supersonic to subsonic. Particles that travel across the shock front increase entropy (nT) from super to sub sonic sides, and decrease flow speed (<v>) from super to sub sonic sides. Shocks affect properties of the system such as density, temperature, or pressure, among other things [Source: Encyclopedia Britannica]. In the case of MSX, the displacement of the particles affected by the shock wave in the system is non-linear in time. What are collisionless-shocks? In MHD plasmas, the nominal collision times are much longer than the transit time for particles across the shock front. Obviously some type of energy and entropy transfer occurs, but it is not due to the usual binary particle-particle collisions that we usually invoke for collisional processes. In MHD it is thought to be due to multiple transits, bounces, re-transits of particles that cross and re-cross the shock. Particles likely interact with waves, and turbulent magnetic structures upstream and downstream from the shock.

ii. What is the motivation behind MSX?

We will apply the knowledge and physical insight gained from these investigations to the development of a working nuclear fusion reactor for sustainable energy. LANL is partnering with the Kirtland Air Force Research Laboratory (AFRL) in this pursuit. AFRL utilizes an almost identical machine to form a field-reversed configuration plasma. However, AFRL translates this plasma into an aluminum flux conserving shell (liner) that subsequently implodes as a result of applied currents and magnetic fields causing a Lorentz force to compress the aluminum liner onto the plasma. The resulting heating and pressurization of the plasma causes the plasma to reach fusion-enabling conditions. The results of investigations into collisionless-shocks will not only give us insight into new physics for fundamental science research, but also will offer insight into the shock waves caused by the imploding aluminum liner and their interaction with the plasma contained within the aluminum liner.

iii. How does MSX work?

Below are two diagrams illustrating the formation and the acceleration stages of the field-reversed configuration plasma in MSX, respectively.

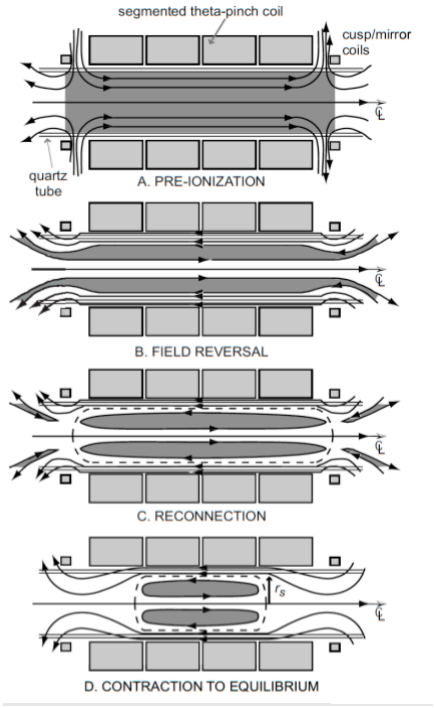

[Source: Rossi]

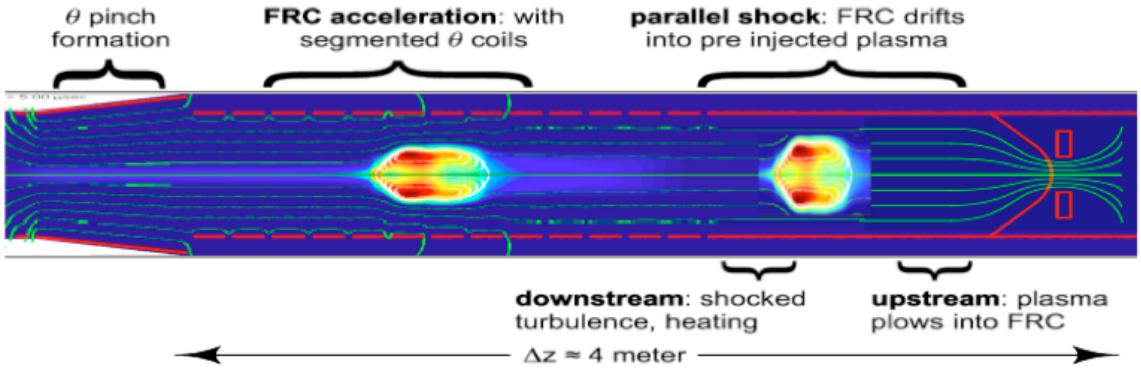

[Source: Intrator]

b. *Brief description of how an interferometer works*

The basic operation of a Mach-Zehnder interferometer starts with the input of a laser beam. The beam is split into two beams. One of these two beams, called the reference beam, passes through a control medium, such as a vacuum or air. The other beam, called the scene beam, passes through the experimental medium, which in this case is plasma. The scene beam and the reference beam undergo different amounts of phase shift during their travels since the amount of phase shift scales proportionally to the line integral of the refractive index through which the beam traverses. From this phase shift information, we are able to calculate the line-integrated density of the plasma.

c. *Significance of the application of this interferometer to MSX*

Application of this interferometer to MSX will enable us to determine the line-integrated density of the plasma in the formation region inside of the theta coils as well as in the translation and shock region.

Among the benefits offered by the interferometer is that it is portable, giving flexibility for remote positioning of the interferometer from the MSX apparatus. The optical fibers can be run dozens of meters from the interferometer apparatus to the MSX apparatus, and so the interferometer can be stored in a remote location such as the MSX screen room, in which the interferometer's detection electronics are shielded from electromagnetic noise emanating from the MSX.

2. Experiment

a. *Description of apparatus and its component parts*

Much of the equipment applied to this experiment was used by two previous NUF program participants while they worked on the interferometer. For further details on their work, see the NUF reports by Oberto and Rossi. However, some of the equipment had been swapped with other equipment since the worked on this experiment. Following are descriptions of the equipment used in the experiment.

Below is a picture of the apparatus.

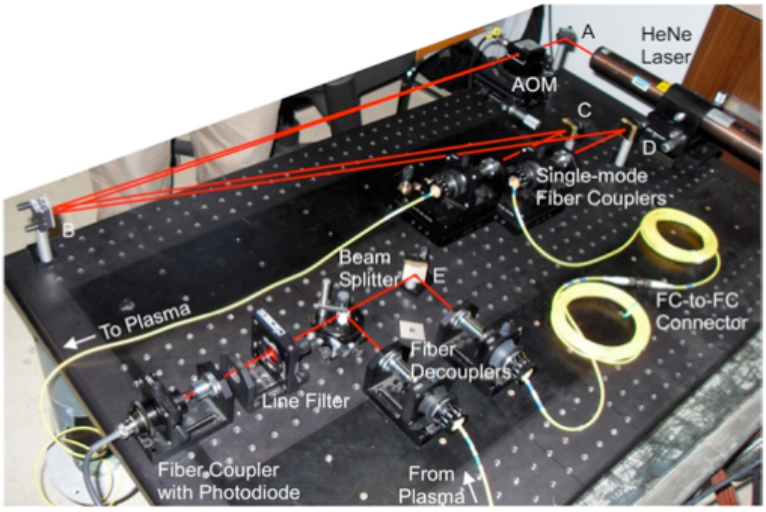

[Source: Oberto]

The interferometer is located on an optical table.

For the production of the laser, we used a 4.5 mW Helium Neon (HeNe) laser operating at 632.8 nm, corresponding to the color red in the visible spectrum. This laser is a Class 3R laser, meaning that its rated power is less than 5 mW. This is convenient in that it is much less administratively restrictive from a safety standpoint than is a Class 3B laser, which has a rated power of 5 mW or above. (Company: Hughes Aircraft Company. Model number: 3225H-PC. Year of manufacture: 1982. Serial Number: 2080102)

An Acousto Optic Modulator (AOM) produced the splitting of the original single laser beam to produce two beams, a zeroth order beam used as the scene beam and a first

order beam used as the reference beam. (Company: NEOS. Model number: 24080. Serial Number: 10905.) The AOM was powered by an AOM Driver. (Company: NEOS. Model Number: 21080-1SAS. Serial Number: 11161)

The course of the laser on the optical table was controlled by the use of five mirrors. (Company: Newport. Model number: MM-1)

Beam blocks were incorporated into the apparatus to serve as an engineering control for safety. They were placed behind and to the sides of the mirrors to prevent possible major reflections of the laser beam off of the optical table.

In order to couple the two laser beams into the fibers, we used fiber mounts to hold microscope objectives and optical fibers in the right alignment. (Mount Company: Newport) (Microscope objectives company: Newport. Model number: M-10X. Characteristics: 10x magnification. 0.25 numerical aperture. 16.5 mm focal length. 7.5 mm clear aperture) (Optical fibers Company: Thorlabs. Model Number: SM 600)

Once the scene and reference beams have traversed the entire course of their separate respective paths, they are mixed, or combined, together using a beam-splitter cube. (Beam-splitter cube Company: Thorlabs. Model Number: BS010). This cube provides for 50% parallel transmission and 50% perpendicular reflection of the laser beam in one perpendicular direction and is anti-reflection coated in the 800 nm range. [Source: Oberto] The combined beam then passes through a line filter which filters out contaminant light at wavelengths other than the wavelength of the laser beam. (Line filter Company: Thorlabs. Model Number: FL632.8-1) [Source: Oberto]

Finally, the mixed laser beam enters into the interferometer's detection circuit, as shown below.

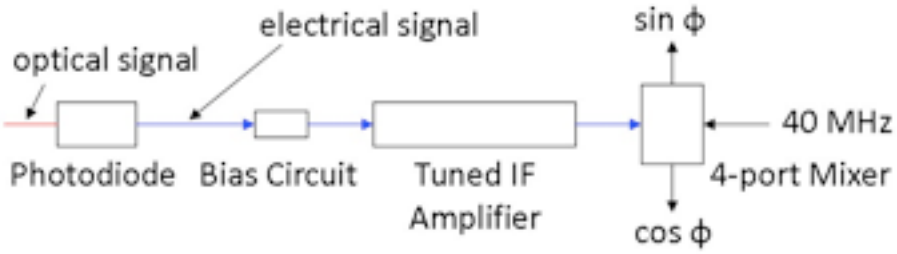

[Source: Oberto]

The ultimate purpose of the interferometer's detection circuit is to extract a signal representing the amount of phase shift that the scene beam has experienced while travelling through the plasma relative to phase shift that the reference beam while travelling through the control medium of air.

This process is split into multiple steps. First, a photodiode converts the optical signal, i.e. the laser beam in electromagnetic form, into an electrical signal. The photodiode is reverse-biased, as explained below. Since the power of the starting laser beam is 4.5 mW, a low to medium powered laser for use in an interferometer, and since the beam is attenuated while traversing its course, the electrical signal must be amplified in order for an obvious signal to be shown on the oscilloscope used in the detection circuit. A Radio Frequency (RF) amplifier (Company: Avantek. Model Number: UTC-102-1. Operating range: 20-150 MHz. Serial Number: 8936SN02.) amplifies the radio frequency electrical signal put out by the photodiode. This electrical signal oscillates in the radio frequency spectrum and thus is amplified by the RF amplifier while electrical

noise that falls outside of the radio frequency spectrum is not amplified, thus increasing the signal to noise ratio. The voltage input into the amplifier should be kept below 10mV to keep the amplifier from burning out. For instance, if applying a test signal to the RF amplifier using a function generator, keep the attenuation of the function generator's output as high as possible.

Low pass filters (Company: Mini-Circuits. Model Number: SBP-70) filter out low frequency mechanical vibration noise from the electrical signal. This noise can be caused by slight movement of any of the pieces involved in the interferometer apparatus, or of vibrations on the MSX vacuum chamber that subsequently vibrate the optical fibers if the optical fibers are mechanically coupled to the vacuum chamber. High pass filters (Company: Newport. Model Number: BLP-21.4) filter out high frequency electrical noise from the electrical signal. This noise can be caused by the operation of other electronic equipment in the vicinity of the interferometer, or by loops of wire used in the interferometer apparatus from emanating stray electromagnetic radiation.

A variable attenuation RF attenuator (Company: Texscan Instruments. Model number: TA-50. Characteristics: 50 ohms, 10 dB, 11 PR) splits the 80 MHz sinusoidal signal emanating from the AOM driver, sending a configurable portion of the signal to the AOM and a much smaller also configurable portion of the signal into the mixer circuit. An I&Q circuit, composed of four electronic devices (Company: KDI Electronics. Model numbers: PSK-213 (two of these), MLK-103M (two of these)) takes as input the electrical signal from the RF amplifier and the 80 MHz electrical signal from the RF attenuator. Ultimately, it puts out two output signals corresponding to the sine and cosine of phase shift.

3. Physics and Mathematics of the apparatus

a. *Mirrors*

Reflections of the laser beam off the mirrors are described by Snell's Law, where $n_1\sin(\theta_1) = n_2\sin(\theta_2)$, n_1 is the index of refraction of air, θ_1 is the angle of incidence, n_2 is the index of refraction of the mirror, and θ_2 is the angle of reflection.

The mirrors used in the interferometer were observed to cause a 0.7 to 0.8 mW decrease in the power of the 4.5 mW laser beam due to diffuse reflections from the mirror surface. 3.8 mW out of the AOM became 3.0 mW off of Mirror B, and with the AOM off, became 2.3 mW off of Mirror D.

b. *Why use an AOM instead of a beam-splitter cube to split the laser beam?*

i. *Principle of operation of the AOM and AOM Driver:* Inside of the AOM is a glass plate that oscillates at a frequency set by the AOM driver. The AOM Driver output signal can be configured to oscillate at frequencies in the range 75 MHz to 85 MHz. For this experiment, the output signal was set to oscillate at 80 MHz. The oscillation of the glass plate in the AOM allows part of the input laser beam to traverse through unaffected. The unaffected output beam is called the zeroth order beam. However, the oscillation of the glass plate in the AOM frequency-shifts part of the input laser beam. This frequency-shifted component of the laser beam is called the first order beam. The first order beam is frequency-shifted upwards by an amount equal to the frequency of oscillation of the AOM's glass plate. In this case, the upward frequency shift is 80 MHz.

ii. *Heterodyne vs. homodyne methods:* One might reasonably ask why it is necessary or beneficial to use the AOM to split the laser beam into two beams, rather than using a beam-splitter cube to do so. The answer to this question is based on the concept of heterodyning. This interferometer is of the heterodyne type. Heterodyning refers to the process of "generating new frequencies by mixing two or more signals" (SEAS). When the AOM operating at 80 MHz is used to frequency shift the laser beam, then even if the phase shift to the scene beam is zero, the electrical signal will contain an oscillation with a frequency of 80 MHz. This is the case in a heterodyne interferometer. On the other hand, in the case of using a beam-splitter cube to split the laser beam, if there is no phase shift in the scene beam, then the frequencies of the scene and reference beams will be equal and the output signal will have a frequency of zero. This is the case in a homodyne interferometer. The main issue with the homodyne method is that it is difficult to determine whether the frequency shift of the scene beam is positive or negative. "Both give output with frequency |delta(w)|. This is the cause of the ambiguity of phase change direction" [Source: Hutchinson]. The benefit of heterodyne operation is that when a phase shift, or equivalently a frequency shift since w = dphi/dt, occurs in the scene beam, the resulting electrical signal in the detection circuit has a frequency of 80 MHz + dphi/dt. Therefore, as long as dphi/dt is less than 80 MHz in magnitude, which is the case in this experiment, the frequency of the electrical signal will always be positive. By observing increases or decreases in the frequency of this electrical signal, one can tell whether the phase shift is in the positive or the negative direction, respectively.

c. Optical fibers

For information on the physical significance of using single-mode fibers, please see Rachel Oberto's NUF report.

d. Photodiode

i. Equations for intensity of light on the photodiode: The intensity of the combined laser beams onto the photodiode can be described by the following equations:

Let D represent sum of the transverse displacements of the oscillating electromagnetic wave from the axis of their propagation.

$$D = ae^{i(\omega_1 t + \phi)} + be^{i\omega_2 t} \quad D^* = ae^{-i(\omega_1 t + \phi)} + be^{-i\omega_2 t}$$

Let the first exponential term represent the zeroth order beam, which serves as the scene beam, and the second exponential term represent the first order beam. Let w1 equal the frequency of the original laser beam, f represent the phase shift undergone by the scene beam, w2 = w1 + 80 MHz. Let a represent the amplitude of the zeroth order beam and b represent the amplitude of the first order beam.

The intensity of the laser beam on the photodiode scales as this displacement term D squared. Since D is complex, we multiply D by its complex conjugate D* rather than squaring D in order to obtain a real product rather than a complex product.

$$
\begin{aligned}
D^*D &= (a\epsilon^{-i(\omega_1 t+\phi)} + b\epsilon^{-i\omega_2 t})(a\epsilon^{i(\omega_1 t+\phi)} + b\epsilon^{i\omega_2 t}) \\
&= a^2 + ab\epsilon^{i(\omega_1 t+\phi)-i\omega_2 t} + ab\epsilon^{i\omega_2 t - i(\omega_1 t+\phi)} + b^2 \\
&= a^2 + b^2 + ab\cos[(\omega_1 - \omega_2)t + \phi] - ab\, i \sin[(\omega_1 - \omega_2)t + \phi] + ab\cos[(\omega_2 - \omega_1)t - \phi] - ab\, i \sin[(\omega_2 - \omega_1)t - \phi] \\
&= a^2 + b^2 + ab\cos[(\omega_1 - \omega_2)t + \phi] - ab\, i \sin[(\omega_1 - \omega_2)t + \phi] + ab\cos[(\omega_2 - \omega_1)t - \phi] + ab\, i \sin[(\omega_1 - \omega_2)t + \phi] \\
&= a^2 + b^2 + ab\cos[(\omega_1 - \omega_2)t + \phi] + ab\cos[(\omega_2 - \omega_1)t - \phi]
\end{aligned}
$$

Making use the trigonometric identity abcos[c + d] + abcos[c - d] = 2abcos[c]cos[d], where $c + d = (w_2 - w_1)t - \phi$, $c - d = (w_1 - w_2)t + \phi$, and thus $2c = c = 0$, and $d = (w_2 - w_1)t + \phi$:

$$
\begin{aligned}
D^*D &= a^2 + b^2 + 2ab\cos[c]\cos[d] \\
&= a^2 + b^2 + 2ab\cos[(\omega_2 - \omega_1)t + \phi] \\
&= a^2 + b^2 + 2ab\cos[(\omega_1 + 80\ \text{MHz} - \omega_1)t + \phi] \\
&= a^2 + b^2 + 2ab\cos[(80\ \text{MHz})t + \phi]
\end{aligned}
$$

In a physical sense, the result obtained above for D*D means that in the detection circuit, we will see a voltage reading that is Direct Current (DC) shifted upwards by a voltage proportional to $a^2 + b^2$. On top of this DC voltage bias there will be an oscillation of amplitude proportional to the product "ab" and with a frequency of 80 MHz.

e. *Purpose of bias circuit*

Forward-biased diodes receive electrons at their anode and discharge electrons at their cathode. The electrical potential of the anode is greater than that of cathode. Electrons will thus flow from anode to cathode. In the reverse-bias configuration, electrons must travel up a potential hill. The bias circuit enables electrons to jump up the potential hill. Essentially, the bias circuit decreases the potential hill that the electrons must climb from cathode to anode. [Source: Sloan] Forward current, i.e., from cathode to anode, in the photodiode causes the emission of light. Absorption of light by the photodiode causes a reverse current, i.e., from anode to cathode.

Benefits of using a bias circuit include improved photodiode response speed and linearity as a result of decreased junction capacitance. However, the system's dark current and noise will increase. [Source: Thorlabs]

Below is the bias circuit recommended for the Thorlabs FGA21 photodiode, which looked most similar to the photodiode of unknown origin and unknown model inherited from previous users of this interferometer apparatus.

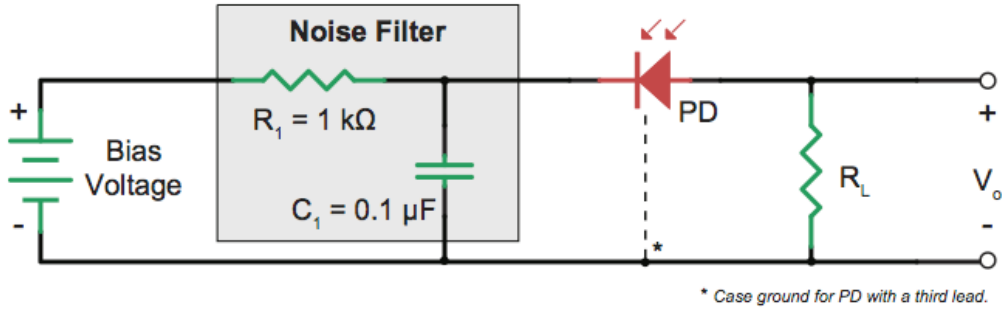

Recommended Bias Circuit for the Thorlabs FGA21 Photodiode [Source: Thorlabs]

f. Mathematics of detection circuit

i. I&Q detection process: Following is a schematic of the basic detection process utilized by the interferometer's detection circuit.

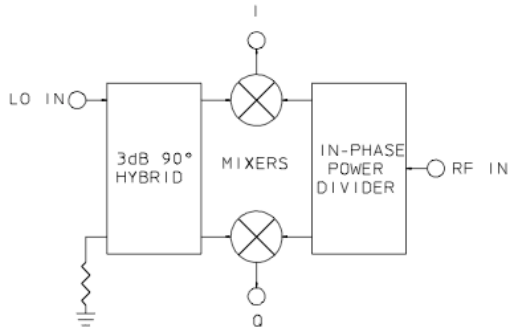

The Basic I & Q Network [Source: Merrimac]

LO stands for local oscillator, in this case the 80 MHz signal from the AOM. RF stands for radio frequency, in this case the photodiode's electrical output that has been amplified by the RF amplifier. I and Q are sinusoidal waveforms phase-shifted from one another by 90 degrees. They contain the phase shift information of the laser beam.

ii. Extraction of phase shift information from the electrical signal: Following is a mathematical derivation for the extraction of the laser beam's phase shift information as carried out by the I & Q detection network:

We start out with a signal whose voltage can be described by:

$$a^2 + b^2 + 2abcos[(80\ MHz)\,t + \phi]$$

First AC couple the signal so that the $a^2 + b^2$ terms disappear:

$$2abCos[80MHz*t + \phi]$$

Then multiply this with the local oscillator signal whose frequency is 80 MHz:

$$2abCos[80MHz*t + \phi]*Cos[80MHz*t + \rho]$$

where the second term represents the local oscillator signal coming from the AOM driver. Let the phase shift, f, in the second term equal zero, since it represents the shift of the local oscillator signal from the AOM driver into the mixer relative to the signal from the AOM driver into the AOM.

$$2abCos[80MHz*t + \phi]*Cos[80MHz*t]$$

Using the trigonometric relation 2Cos[f]Cos[g] = Cos[f - g] + Cos[f + g], and letting f = 80MHz*t + ϕ and g = 80MHz*t, we obtain the following result:

$$\frac{1}{ab}(Cos[80MHz*t + \phi - 80MHz*t] + Cos[80MHz*t + \phi + 80MHz*t])$$

$$\frac{1}{ab}(Cos[\phi] + Cos[160MHz*t + \phi])$$

The particular mixer used in this interferometer also mixes the electrical signal from the photodiode with a local oscillator signal that has been phase shifted by 90 degrees:

$$2abCos[80MHz*t + \phi]*Sin[80MHz*t]$$

Using the trigonometric relation 2Sin[f]Cos[g] = Sin[f - g] + Sin[f + g], and letting f = 80MHz*t + ϕ and g = 80MHz*t, we obtain the following result:

$$\frac{1}{ab}(\text{Sin}[80\text{MHz}*t + \phi - 80\text{MHz}*t] + \text{Sin}[80\text{MHz}*t + \phi + 80\text{MHz}*t])$$

$$\frac{1}{ab}(\text{Sin}[\phi] + \text{Sin}[160\text{MHz}*t + \phi])$$

The low-pass filters included in the final portion of this interferometer's detection circuit block out the sine and cosine output signals oscillating at 160MHz. Therefore, the outputs of the mixer are the sine and cosine of the phase shift, ϕ, caused by the plasma in the scene beam path. This combination of the sine and the cosine of the phase shift gives us an unambiguous view of the direction and magnitude, up to but not over 360 degrees, of the phase shift.

iii. Relation between plasma density and plasma phase shift information:

$$\Delta\phi = \int_0^R k\, dl$$

where ϕ is the phase shift, k is the plasma's index of refraction, and dl is the infinitesimal length along the interferometer's view chord of sight through the plasma. [Source: Hutchinson]

iv. Abel-Inversion: In order to transform our knowledge of the plasma density along the height y, as seen in the below diagram, to a function of the radius r, we make use of the Abel Transform.

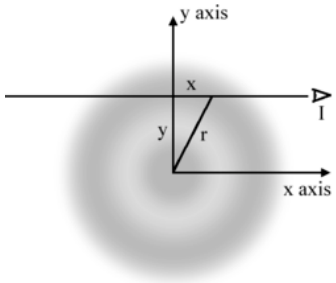

Visualization of the Abel Transform [Source: Wikipedia]

The Abel Transform can be expressed as follows:

$$S(y) = 2*\int_y^R f(r)\left(r^2 - y^2\right)^{-\frac{1}{2}}\, r\, dr$$

where S(y) represents the plasma density along line x at height y in the above diagram. f(r) represents the plasma density as a function of the plasma radius r.

The inverse formula can be expressed as follows:

$$f(r) = -\frac{1}{\pi}\int_r^R \frac{\partial S(y)}{\partial y}\left(y^2 - r^2\right)^{-\frac{1}{2}}\, dy$$

[Source: Kalal]

We now have a function for the plasma density as a function of radius. Adding more view chord lines of sight that we are able to obtain by increasing the number of scene beams through the plasma allows us to obtain a greater a picture of the plasma density as a function of the plasma radius.

v. Residual phase differences: Phase differences between the reference and scene beams may be caused by factors other than the presence of a material such as plasma in the path of the scene beam. If the lengths of the reference and scene beams are not equal, there will be a phase difference between the two beams upon their subsequent recombination. In order to minimize phase difference caused by path-length differences, the lengths of these two paths should be as close to equal as possible. As a rule of thumb, the difference in length between the two paths should, at the very least, be shorter than the length of the laser's optical resonator.

g. Sources of Noise

Possible sources of noise in the apparatus include: 1. High frequency noise due to the coupling of electromagnetic fields from one part of the interferometer apparatus to another. As a specific example, currents in BNC cables and power cords all sharing the same ground will form ground loops. As visualized through use of the right-hand rule for electric and magnetic fields, the flow of current in these ground loops produce magnetic fields, which can cause noise in the detection electronics. 2. Low frequency mechanical vibrations from equipment such as beam choppers, nearby pumps used on MSX, and vibrations coupled between the MSX vacuum chamber and optical fibers potentially mounted on the vacuum chamber.

4. Results

a. Testing and troubleshooting

It was discovered that the RF amplifier does not work. A function generator was used to send a periodic signal, in particular a sinusoid, into the RF amplifier at a frequency of about 25 MHz. While the function generator's signal was observed on the oscilloscope, the output of the RF amplifier showed a very feeble and highly distorted sinusoid. This indicated that the RF amplifier was not properly amplifying the input signal wave, of only a few millivolts in amplitude.

When the circuit was not reverse-biased, the direct output of the photodiode showed no signal corresponding to the laser beam with intensity of approximately 100 uW shown onto the photodiode. Rather, there was lots of noise on the order of 1 mV peak-to-peak. Under the assumption that the photodiode required a reverse bias in order to function properly, a reverse bias circuit was assembled on a breadboard. However, the photodiode still showed no response to the incoming laser beam.

A new photodiode (Company: DIGI-KEY. Part Number: PN334PA-ND. Manufacture Number: PN334) replaced the broken photodiode. Illuminating the photodiode with a flashlight caused a recognizable signal on the oscilloscope, verifying that this new photodiode worked.

Use of a power meter operating in the visible spectrum allowed us to measure the output power of the reference beam. The maximum power throughput was recorded at 452 uW. The transmitted power can go above this, but increasing the power transmission was not pursued at the time since personnel efforts turned to working on the detection circuit, which should work with this level of power.

b. Experimental results

In order to test the detection circuit without depending upon high energy transmission through the optical fibers, the author removed the optical fibers from the apparatus. The mirrors were used instead of the fibers to direct the laser beams onto the photodiode. Applying the direct output of the photodiode to the oscilloscope without using the detection circuit, and with the AOM driver frequency at half range and its power output at half range, the following observations were noted:

The zeroth order beam was observed to be a relatively flat 400 mV signal with small non-periodic ripples superimposed onto it.

The first order beam was observed to be a square wave of 200 mV peak-to-peak amplitude with a period of 20 ms. Small non-periodic oscillations of peak-to-peak amplitude approximately 1 mV were superimposed onto the square wave.

The combined zeroth and first order beams were observed to be a relatively flat 400 mV signal.

The expected sinusoidal oscillation in the range 75 MHZ – 85 MHZ was not observed, likely indicating a mechanical issue in the apparatus. Possible sources of error include an improperly functioning AOM or an energy imbalance between the zeroth and first order beams. A possible source of the former issue is that the AOM is susceptible to damage by laser beams improperly aligned with its entrance and exit apertures, which can burn out the AOM's interior components. The AOM driver was tested and shown to be working, putting out square waves in the 75 MHz – 85 MHz range.

Further work is needed to ensure that all parts of interferometer apparatus, including the AOM and the detection circuit, are functioning properly, to produce and assemble a data acquisition (DAQ) system to analyze the electrical output from the I&Q network, and a structure that will hold the optical fibers in position near the MSX vacuum chamber without necessitating mechanical coupling between the fibers and the chamber. The interferometer will then be applied to the Magnetized Shock Experiment.

5. Conclusion

The multi-chord heterodyne fiber optic Mach-Zehnder interferometer will be applied to the Magnetized Shock Experiment (MSX) at Los Alamos National Laboratory to measure plasma density remotely. Upon the implementation of several such fiber sets, the apparatus will be used to determine the line-integrated density of the plasma from many different view chords. We will then Abel invert the acquired data to provide radially resolved spatial profiles of the plasma density.

6. Acknowledgements

This work was supported by DOE Office of Fusion Energy Science under LANS Contract DE–AC52-06NA25369, NNSA, LANL, and the PPPL National Undergraduate Fellowship Program.

The author would like to thank the following Plasma Physics scientists for their guidance and support of this research: Dr. Thomas Intrator, Dr. Thomas Weber, Dr. Jason Sears, Mr. Soonwook Jung, Mr. John Dunn, Ms. Liz Merrit, Dr. Auna Moser, Dr. Glen Wurden, and Dr. Scott Hsu.

7. References

1. Encyclopedia Britannica Online. “Shock Wave”. http://www.britannica.com/EBchecked/topic/541339/shock-wave/. (2012)

2. Hutchinson, I. H. “Principles of Plasma Diagnostics”. Cambridge University Press. (1987)

3. Intrator, T. P.; Weber, T. “Magnetized shock studies for HEDP and astrophysics using a plasmoid accelerator”. (2011)

4. Jones, V. R. “The Heterodyne “Principle””. http://people.seas.harvard.edu/~jones/cscie129/nu_lectures/lecture7/heterodyne/heterodyne.html. (2004)

5. Kalal, Milan; Nugent, Keith A. “Abel inversion using fast Fourier transforms”. Applied Optics. Vol. 27, No. 10. (1988)

6. Merrimac Industries. “Complex Modulators and Demodulators”. http://www.merrimacind.com/rfmw/02intro_modulators.pdf. (1996)

7. Oberto, R. “Development of a Fiber Interferometer for the FRX-L Experiment”. NUF Report. (2009)

8. Rossi, G. D. “MTC-FRC Optimization & 3D Plasma Reconnection Mapping via Single Mode Interferometry”. NUF Paper. (2010)

9. Slone, R. “TAB Electronics Guide to Understanding Electricity and Electronics”. The McGraw-Hill Companies, Inc. (2000)

10. Thorlabs. “FGA21 Photodiode Product Specification Sheet”. http://www.thorlabs.com/Thorcat/13800/FGA21-SpecSheet.pdf. (2011)

11. Wikipedia. “Abel Transform”. http://en.wikipedia.org/wiki/Abel_transform. (2012)